tropages at the larger scales, which suggests a common source of variability (probably physical).

Video data acquisition for plankton makes possible immediate, in situ observation of dominant taxa; such visual observations allow instant qualitative assessment of taxonomic composition in plankton communities. Given recent advances in video image processing including real-time digitization, thresholding, convolutions, and edge detection (12), real-time sorting of plankton into taxonomic categories will be possible in the near future. This will allow rapid quantitative mapping of plankton abundance together with taxonomic and size composition. Rapid acquisition of size-dependent taxonomic data over a range of scales in a dynamical oceanographic environment will provide new insights into the biological and physical processes controlling plankton populations in the sea.

REFERENCES AND NOTES

1. B. J. Rothschild and C. G. H. Rooth, *Cooperative Institute for Marine and Atmospheric Studies Technical Report No. 82008* (University of Miami, Miami, FL, 1982).
2. Marine Zooplankton Colloquium, *Mar. Ecol. Prog. Ser.* 55, 197 (1989).
3. W. J. Vlymen, *Environ. Biol. Fishes* 2, 211 (1977).
4. C. S. Davis, G. R. Flierl, P. H. Wiebe, P. J. S. Franks, *J. Mar. Res.* 49, 109 (1991).
5. M. R. Reeve, *J. Plankton Res.* 2, 381 (1980).
6. Field data on spatial relationships among individual planktonic organisms are rare. Some statistical evidence for the existence of plankton micropatchiness has been obtained with a towed bottle sampler [R. W. Owen, *J. Mar. Res.* 47, 197 (1989)], but limited bottle number (15) and potential avoidance problems prevented estimates of patch size structure and interneighbor distances. Direct observations of certain larger pelagic organisms (>1 cm) such as medusae and krill have been made with the use of scuba and submersibles [C. E. Mills and J. Goy, *Bull. Mar. Sci.* 43, 739 (1988); W. M. Hamner, P. P. Hamner, B. S. Obst, *Limnol. Oceanogr.* 34, 451 (1989)], but direct observation and quantification of smaller organisms (<1 cm; that is, the bulk of the plankton) have proven difficult. Rough estimates of macrozooplankton (that is, ~3-mm *Calanus* sp.) abundance (number of organisms per square meter) have been obtained from a limited number of visual observations made with manned submersibles with a ruler mounted outside the viewing window. Avoidance problems and inability to see smaller plankton have made it difficult or impossible to use such systems for quantitative assessment of most plankton [A. L. Alldredge *et al.*, *Mar. Biol.* 80, 75 (1984); G. O. Mackie and C. E. Mills, *Can. J. Fish. Aquat. Sci.* 40, 763 (1983)]. High-magnification cinematographic observations of copepods have been made in the laboratory [J. R. Strickler, *Science* 218, 158 (1982)]. More recently, vertical distributions of doliolids in the field were quantified with a low-magnification video camera (20-cm field) mounted on a submersible [G.-A. Paffenhöfer, *J. Plankton Res.* 13, 971 (1991)]. Observation of plankton in situ at high magnification (<5 mm) has been difficult as a result of the relatively rapid motions and resultant image smearing at these scales.
7. The VPR consists of four video cameras with magnifying optics that we set for concentric viewing fields of 0.68, 1.78, 5.38, and 9.25 cm. Corresponding volumes were 0.9, 19.8, 200.0, and 636.4 ml (±5%). The VPR is towed such that the

flow is orthogonal to the camera-strobe axis. Resolution in the high-magnification viewing field was measured to be 10 µm. An 80-W xenon strobe (pulse duration = 1 µs) was synchronized to match the video sampling rate of 60 fields per second. A long-pass, sharp-cut filter (>590 nm) was used on the strobe light to minimize risk of detection by plankton. The red light beam was expanded to 10 cm, collimated, and aimed obliquely past the cameras to provide dark-field illumination. Strobe to camera distance was 1.0 m with the viewing area at 0.5 m. Video data were telemetered to the surface via fiber-optic cable and stored, together with time code overlay, by the use of broadcast-quality video tape recorders. The VPR design is fully described elsewhere [C. S. Davis, S. M. Gallager, M. S. Berman, L. R. Haury, J. R. Strickler, *Arch. Hydrobiol.*, in press]. To minimize potential avoidance problems (8), we did not incorporate the gauze recorder box into the VPR, so that the 1.0-m space between the cameras and the strobe was free of obstructions.
8. The VPR was designed to minimize disturbance of the sampled volume in order to reduce possible disruption of the imaged particles or detection and avoidance by the plankton. Frontal area is much smaller than that of a comparably sized (1 m²) plankton net, and the imaged volume is located along the forward (upstream) edge of the instrument. Red light was used because zooplankton are known to be phototactic but are least sensitive to long wavelengths of light [K. V. Singarajah, *J. Mar. Biol. Assoc. U.K.* 55, 627 (1975); J. H. Blaxter, *J. Exp. Biol.* 41, 155 (1975)]. The large amount of open space between cameras and strobe (1.0 m) minimizes flow disturbance near the viewing area as determined by dye and avoidance studies in a tow tank [C. S. Davis and L. Haury, unpublished data]. In situ observations made in lower magnification cameras revealed that the organisms' trajectories, body orientation, and shape remained constant during transit through these windows, which indicates lack of flow distortion or escape response.
9. E. J. Carpenter and K. Romans, *Science* 254, 1356 (1991); D. G. Capone and E. J. Carpenter, *ibid.* 217, 1140 (1982); E. J. Carpenter, *Mar. Biol. Lett.* 4, 6 (1983).
10. D. Deibel, *J. Mar. Res.* 43, 211 (1985); *J. Plankton Res.* 4, 143 (1982); *ibid.*, p. 189.
11. Given the binary nature of the data, standard spectral techniques using Fourier series could not be used to quantify variability as a function of spatial scale. The point process method used involved estimating the mean density of organisms at a distance, *h*, away from an individual [D. R. Cox and P. A. W. Lewis, *The Statistical Analysis of Series of Events* (Chapman and Hall, London, 1978)]. This was repeated for a range of *h* values to obtain a patchiness index as a function of length scale, $P(h)$. Patchiness indices were calculated separately for length scales of 1, 10, and 200 m. Confidence intervals (95%) were determined by calculating the patchiness index for each of 100 simulated random distributions. We found confidence intervals for 1- and 10-m scales by first smoothing the data with 8- and 80-m band widths, respectively, and then determining the patchiness index from simulations that randomized the smoothed data over length scales of 1 and 10 m. In this way, the patchiness index at smaller scales was unaffected by patchiness at larger scales. This method was also used across taxa to estimate correlations in abundance.
12. M. S. Berman, C. Katsinis, H. P. Jefferies, R. Lambert, *Eos* 71, 94 (1990).
13. Supported by NSF grant OCE-9012657. We thank J. Kinder, P. Alatalo, B. Flannery, L. Haury, M. Gould, W. Lange, T. Silva, J. Strickler, the *Oceanus* crew, and the Woods Hole Oceanographic Institution (WHOI) facilities and graphics personnel for their inputs. We especially thank A. Morton, Sea Scan, Inc., North Falmouth, MA, for manufacturing the VPR according to our design. WHOI contribution 7928.

4 March 1992; accepted 18 May 1992

Megascopic Eukaryotic Algae from the 2.1-Billion-Year-Old Negaunee Iron-Formation, Michigan

Tsu-Ming Han and Bruce Runnegar*

Hundreds of specimens of spirally coiled, megascopic, carbonaceous fossils resembling *Grypania spiralis* (Walcott), have been found in the 2.1-billion-year-old Negaunee Iron-Formation at the Empire Mine, near Marquette, Michigan. This occurrence of *Grypania* is 700 million to 1000 million years older than fossils from previously known sites in Montana, China, and India. As *Grypania* appears to have been a photosynthetic alga, this discovery places the origin of organelle-bearing eukaryotic cells prior to 2.1 billion years ago.

Megascopic fossils resembling *Grypania spiralis* (Walcott) from the late Proterozoic of Montana (1, 2), China (2, 3), and India (4) occur within the lower part of the Negaunee Iron-Formation (IF), northern Michigan (Figs. 1 and 2). The Negaunee IF (Marquette Range) and correlative Biwabik

IF (Mesabi Range) have given an isotopic date (Sm-Nd isochron) of 2110 ± 52 million years (5) and are early Proterozoic in age. This new horizon predates previously known occurrences of *Grypania* by 700 to 1000 million years; the fossils are the oldest known remains of megascopic organisms.

Grypania spiralis was a corkscrew-shaped, spaghetti-like organism that grew to maximum size of about half a meter in length and 2 mm in diameter (Fig. 3E). It is normally preserved as unbranched, ribbon-like films or impressions on bedding planes, but a unique specimen from India illustrated by Beer (6) is uncompacted, showing

T.-M. Han, Research Laboratory, Cliffs Mining Services Company—Michigan, 504 Spruce Street, Ishpeming, MI 49849.
B. Runnegar, Department of Earth and Space Sciences, Molecular Biology Institute, and Institute of Geophysics and Planetary Physics, University of California, Los Angeles, CA 90024.

*To whom correspondence should be addressed.

that *Grypania* was originally circular in cross section. Rarely seen terminations are rounded; well-preserved specimens from India and China have transverse markings (*2, 4*), which are best interpreted as the trace of spiral elements within the wall of the organism (*7*). Thus the corkscrew shape of *Grypania* appears to have been due to supercoiling that was maintained in life and death by helical filaments within the body wall. As a result, *Grypania* is almost always preserved as a compressed coil, sinuous ribbon, or cuspate ribbon. Walter *et al.* (*2*) regarded the cuspate ribbons as specimens of *Grypania* that had been stretched by currents; it was therefore thought that *Grypania* might have been tethered during life.

The Negaunee fossils are from thinly bedded magnetite-carbonate-silicate-chert IF (silicate horizon) in the Empire Mine (*8*). The fossiliferous zone is exposed on the east side of the pit; it is about 335 m above sea level and about 180 to 210 m stratigraphically above the base of the Negaunee IF (Fig. 2). The fossils occur on top of and at the base of 1- to 10-mm-thick magnetite-rich layers. They are abundant, carbonaceous in composition, and are of two main types: coiled, thin filaments resembling *Grypania spiralis* from Montana (Fig. 3, A

to D); and coiled, thicker forms (Fig. 1) that may represent a new genus or species. The thinner forms are coiled or curved, smooth, uniformly wide filaments, 0.7 to 1.1 mm in width, and up to 90 mm in length. Many are preserved as tightly wound coils of three or fewer turns but on some surfaces the filaments lie in irregular, sinuous or cusp-shaped curves (some bedding surfaces are covered with fragments of many different sizes). The coils are typically oval in shape due to post mortem deformation, from 5 to 30 mm in average diameter, and of various sizes on the same surface. Terminations are smoothly rounded except where obviously torn. The thicker forms are wider (about 1.5 mm), more tightly coiled (5 to 9 mm in diameter) and shorter (up to 30 mm), but in other respects are not obviously different from the thinner forms. Neither type shows evidence of transverse markings.

Grypania has no certain living relatives but is regarded as a probable eukaryotic alga because of its complexity, structural rigidity, and large size. Spiral-shaped fossil cyanobacteria known as *Obruchevella* and *Spirellus* are widespread in late Proterozoic and early Cambrian strata (*9*) but even the exceptionally large Cambrian forms (*Spire-*

llus) are orders of magnitude smaller than *Grypania* (Fig. 4). Similarly, it is unlikely that *Grypania* was the abandoned giant sheath of a sulfide-oxidizing bacterium (Beggiatoaceae) as has been suggested for late Proterozoic carbonaceous megafossils known as vendotaenids (*10*); the largest known bacterial sheaths (0.5 mm in diameter) are narrower than large specimens of *Grypania* and they lack rounded ends, a coiled morphology, and transverse structures (*11*). A third possibility, that *Grypania* represents an aggregate of bacterial or cyanobacterial filaments, may also be discarded because even man-made bacterial fibers are less well organized and narrower than *Grypania* (*12*). Natural aggregates of filaments (for example, *Nostoc* colonies) may be cylindrical in form and up to 0.5 mm in width, but they lack structures that could maintain a coiled morphology.

The best modern analog for *Grypania* may be the giant unicellular dasycladacean alga *Acetabularia* (*13*). Before the formation of an umbrella-shaped reproductive cap, *Acetabularia* grows as a narrow cylinder about 0.4 mm in diameter and up to 180 mm in length. The single nucleus remains within a holdfast; there is a large, central, sap-filled vacuole that occupies most of the stalk of the alga so that the cytoplasm, which contains numerous chloroplasts and mitochondria, is restricted to the periphery. Although *Acetabularia* is unicellular, its close relatives have a coenocytic organization, as might have *Grypania*. In summary, *Grypania* is interpreted as a sessile, eukaryotic alga that may have been unicellular but is more likely to have been either multinucleate or multicellular. Few uninucleate organisms have achieved the cytoplasmic volume (~1.5 ml) of Indian specimens of *Grypania* (Fig. 3E). As *Grypania* has no obvious modern counterpart, it may belong to an extinct algal group.

Phylogenetic trees constructed from the sequences of genes that were duplicated before the existence of the latest common ancestor of all living organisms have re-

Fig. 1. Bed surface of Negaunee Iron-Formation with numerous fragments of *Grypania* and some thicker filaments. Line represents 2-cm-wide strip of unfossiliferous rock; coin is 18.5 mm in diameter.
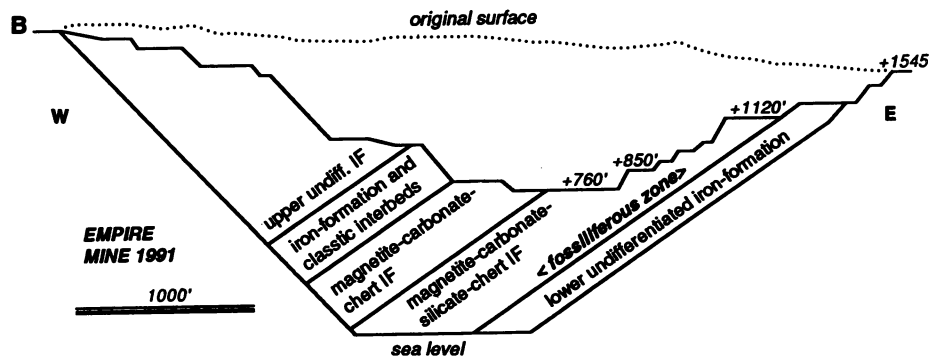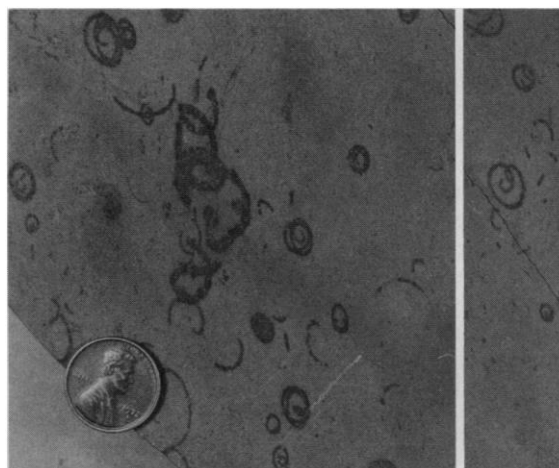

Fig. 2. Locality map and east-west cross section of the Empire Mine showing the 1991 and projected positions of the pit surface.

Fig. 3. (**A** to **D**) Specimens of *Grypania* from the Negaunee Iron-Formation, Empire Mine. (**E**) Large specimen of *Grypania spiralis*, about 1100 million years old, Rohtas Formation, Semri Group, Vindhyan Supergroup, central India. Scale bar in (C) (applies to A to D), 1 cm; scale bar in (E), 1 cm.
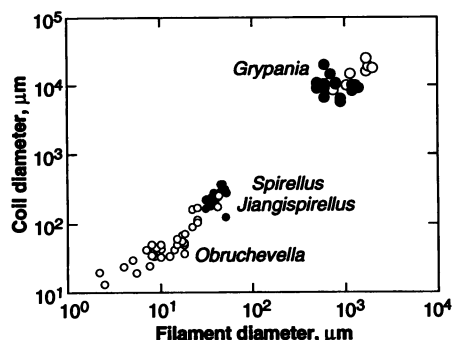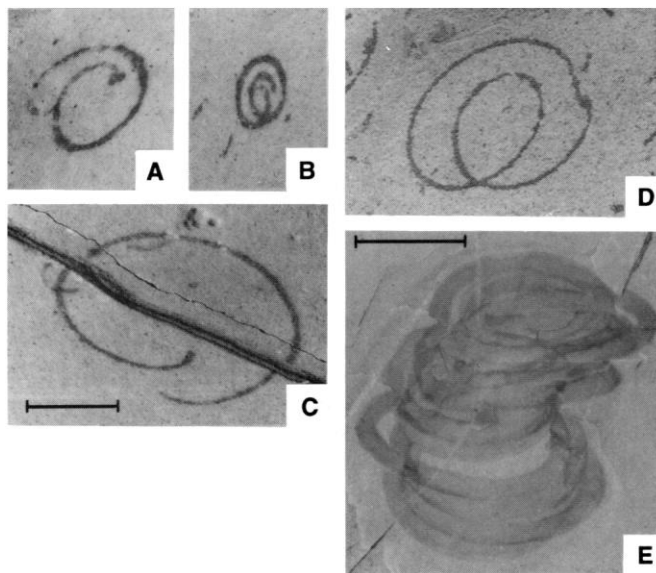

Fig. 5. Cartoon showing the major branches of the universal tree of life and the presumed position of *Grypania* in the tree.

Fig. 4. Scatterplot of sizes of late Proterozoic and Cambrian spirally coiled cyanobacteria (*Obruchevella*, open circles; *Spirellus* and *Jiangispirellus*, solid circles) for comparison with specimens of *Grypania spiralis* (open circles) and *Grypania* from the Negaunee Iron-Formation (solid circles).

vealed that eukaryotes are more closely related to archaebacteria than they are to eubacteria (*14*). Cavalier-Smith (*15*) has described one plausible scenario for the origin of the eukaryotic cell from eubacteria that had lost the ability to manufacture murine-based cell walls and consequently needed an internal cytoskeleton as well as sterols to stiffen cell membranes. He further suggested that the earliest eukaryotes would have lacked mitochondria and chloroplasts as these organelles were acquired by endosymbiosis after the divergence of living amitochondriate protists (for example, *Giardia*) from the line leading to organelle-bearing eukaryotes (*16*).

The time of origin of eukaryotes has been estimated by the maximum sizes of organic-walled microfossils [>1.75 billion to ?2.0 billion years ago (*17*)], carbonaceous megafossils [>1.8 billion years ago (*18*)], biomarker molecules (modified sterols) extracted from Proterozoic rocks

[>1.7 billion years ago (*19*)], and the molecular clock [1.8 billion ± 0.4 billion years ago (*20*)]. If the Negaunee fossils are correctly interpreted as the remains of eukaryotic algae, the origin of organelle-bearing eukaryotes must have occurred prior to 2.1 billion years ago. Although this date is 300 million years older than most previous estimates, it may also underestimate significantly the times of origin of (i) the first stem group eukaryote (latest common ancestor of all living and extinct eukaryotes); (ii) eukaryotic organization (membrane sterols, cytoskeleton, nucleus, Golgi apparatus, mitosis, and so on); (iii) the first crown group eukaryote (latest common ancestor of all living eukaryotes); and (iv) the endosymbiotic conversion of purple bacteria and cyanobacteria into mitochondria and chloroplasts in an early eukaryote (*21*). Each of these events must have taken place in the order given above before about 2.1 billion years ago (Fig. 4).

There is limited geological evidence that points to the existence of stem group eukaryotes in the late Archean (>2.5 billion years ago). By definition, the first stem group eukaryote was either the closest coeval relative of the ancestral archaebacterium, if the Archaebacteria is a monophyletic group (*22*); or the sister species of the first sulfobacterium, if Lake's "eocytes" are the closest prokaryotic relatives of the eukaryotes (*23*). Although the second alternative is supported by new evidence (*24*), the long-standing difficulty of resolving the topology of the node or nodes near the base of the archaebacterial branch of the universal tree is an indication that the principal groups of archaebacteria and the stem group eukaryotes originated at approximately the same time (*25*).
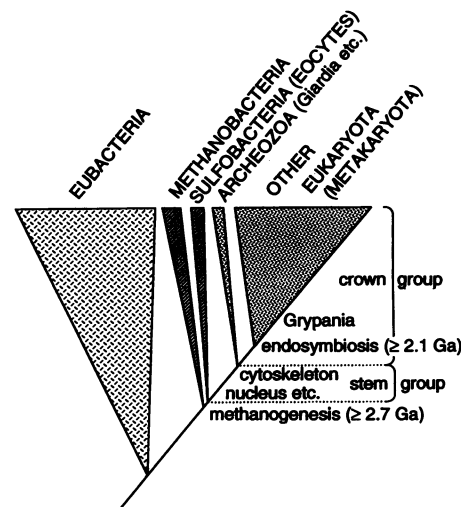
Exceptionally light carbon isotope ratios

($\delta^{13}C_{PDB} \leq -40$ per mil) obtained from organic matter found in late Archean and early Proterozoic rocks (*26*) have been interpreted as evidence for the existence, at those times, of eubacterial methylotrophs that were using methane produced by archaebacterial methanogens (*27*). Thus the original stem group eukaryote may have lived before 2.5 billion to 2.7 billion years ago (Fig. 5). It follows that the divergence between eukaryotes and eubacteria may be much deeper than the about 1.8 billion year date obtained by extrapolating rates of protein evolution (*20*).

The earliest crown group eukaryotes lacked mitochondria and were therefore incapable of aerobic respiration (*15–16*). However, *Grypania* probably respired and consequently needed at least 1% of the present atmospheric level (PAL) of oxygen to survive (*13*). This suggests that oxygen was a significant component of the earth's atmosphere ($\geq 10^{-2}$ PAL O_2) during the main period of banded iron formation deposition, some 2.0 billion to 2.5 billion years ago.

REFERENCES AND NOTES

1. M. R. Walter, J. H. Oehler, D. Z. Oehler, *J. Paleontol.* **50**, 872 (1976).
2. M. R. Walter, R. Du, R. J. Horodyski, *Am. J. Sci.* **290-A**, 133 (1990).
3. R. Du and L. Tian, *Precamb. Res.* **29**, 5 (1985); R. Du, L. Tian, H. Li, *Acta Geol. Sin.* **1986** (2), 115 (1986).
4. Spiral fossils that closely resemble Chinese examples of *Grypania spiralis* have been described from the lower part of the Vindhyan Supergroup (Rohtas Formation, Semi-group) in central India as *Katnia singhi* Tandon and Kumar [K. K. Tandon and S. Kumar, *Curr. Sci.* **46**, 563 (1977); *Geophytology* **7**, 126 (1977)]. The age of the lower Vindhyan Supergroup is not well constrained but appears to be at least 1100 million years old [A. R. Crawford and W. Compston, *Q. J. Geol. Soc. London* **125**, 351 (1971); A. Chakrabarti, *Precamb. Res.* **47**, 141 (1990)].
5. D. C. Gerlach, S. B. Shirey, R. W. Carlson, *Eos* **69**, 1515 (1988).

6. E. J. Beer, *Rec. Geol. Surv. India* 50, 139 (1919).
7. B. Runnegar, unpublished observations.
8. T. M. Han, *U.S. Geol. Surv. Prof. Pap.* 769, 76 (1975).
9. P. Cloud, S. M. Awramik, K. Morrison, D. G. Hadley, *Precamb. Res.* 10, 73 (1979); F. Wang, *Nature* 294, 74 (1981); X. Song, *Geol. Mag.* 121, 179 (1984); R. Riding and L. Voronova, *ibid.*, p. 205; J. S. Peel, *Rapp. Grønlands Geol. Unders.* 137, 5 (1988); A. H. Knoll and Y. Ohta, *Polar Res.* 6, 59 (1988).
10. G. Vidal, *Lethaia* 22, 375 (1989).
11. V. A. Gallardo, *Nature* 268, 331 (1977); C. R. Smith, H. Kukert, R. A. Wheatcroft, P. A. Jumars, J. W. Deming, *ibid.* 341, 27 (1989); H. W. Jannasch, D. C. Nelson, C. O. Wirsen, *ibid.* 342, 834 (1989); M. P. Starr, H. Stolp, H. G. Trüper, A. Balows, H. G. Schlegel, *The Prokaryotes* (Springer-Verlag, Berlin, 1981).
12. N. H. Mendelson, *Proc. Natl. Acad. Sci. U.S.A.* 73, 1740 (1976); _____ and J. J. Thwaites, *J. Bacteriol.* 171, 1055 (1989).
13. B. Runnegar, *Palaeogeogr. Palaeoclimatol. Palaeoecol.* 97, 97 (1991).
14. J. P. Gogarten *et al.*, *Proc. Natl. Acad. Sci. U.S.A.* 86, 6661 (1989); N. Iwabe, K. I. Kuma, M. Hasegawa, S. Osawa, T. Miyata, *ibid.*, p. 9355.
15. T. Cavalier-Smith, *Ann. N.Y. Acad. Sci.* 503, 17 (1987).
16. M. L. Sogin, J. H. Gunderson, H. J. Elwood, R. A. Alonso, D. A. Peattie, *Science* 243, 75 (1989); K. S. Kabnick and D. A. Peattie, *Am. Sci.* 79, 34 (1991).
17. J. W. Schopf, in *Major Events in the History of Life*, J. W. Schopf, Ed. (Jones & Bartlett, Boston, MA, 1992), pp. 29–63.
18. H. J. Hofmann and J. Chen, *Can. J. Earth Sci.* 18, 443 (1981).
19. R. E. Summons, T. G. Powell, C. J. Boreham, *Geochim. Cosmochim. Acta* 52, 1747 (1988); R. E. Summons and M. R. Walter, *Am. J. Sci.* 290-A, 212 (1990).
20. R. F. Doolittle, K. L. Anderson, D. F. Feng, in *The Hierarchy of Life*, B. Fernholm, K. Bremer, H. Jörnvall, Eds. (Elsevier, Amsterdam, 1989), pp. 73–143.
21. T. Cavalier-Smith, *Ann. N.Y. Acad. Sci.* 503, 55 (1987).
22. C. R. Woese and G. E. Fox, *Proc. Natl. Acad. Sci. U.S.A.* 74, 5088 (1977); C. R. Woese, *Microbiol. Rev.* 51, 221 (1987); _____, O. Kandler, M. L. Wheelis, *Proc. Natl. Acad. Sci. U.S.A.* 87, 4576 (1990).
23. E. Henderson, M. Oakes, M. W. Clark, J. A. Lake, A. T. Matheson, W. Zillig, *Science* 225, 510 (1984); J. A. Lake *Nature* 331, 184 (1988); *Mol. Biol. Evol.* 8, 378 (1991).
24. M. C. Rivera and J. A. Lake, *Science* 257, 74 (1992).
25. N. Iwabe, K. I. Kuma, H. Kishino, M. Hasegawa, T. Miyata, *J. Mol. Evol.* 32, 70 (1991).
26. M. Schidlowski, *Nature* 333, 313 (1988).
27. J. M. Hayes, in *Earth's Earliest Biosphere. Its Origin and Evolution*, J. W. Schopf, Ed. (Princeton Univ. Press, Princeton, NJ, 1983), pp. 291–301.
28. We thank J. W. Villar and G. L. LaBerge for their enthusiastic support of this work and the Management of Cleveland-Cliffs, Inc. for permission to publish this paper.

Modulation of DNA Binding Specificity by Alternative Splicing of the Wilms Tumor *wt1* Gene Transcript

W. A. Bickmore, K. Oghene, M. H. Little, A. Seawright, V. van Heyningen, N. D. Hastie*

The technique of whole-genome polymerase chain reaction was used to study the DNA binding properties of the product of the *wt1* gene. The zinc finger region of this gene is alternatively spliced such that the major transcript encodes a protein with three extra amino acids between the third and fourth fingers. The minor form of the protein binds specifically to DNA. It is now shown that the major form of wt1 messenger RNA encodes a protein that binds to DNA with a specificity that differs from that of the minor form. Therefore, alternative splicing within the DNA binding domain of a transcription factor can generate proteins with distinct DNA binding specificities and probably different physiological targets.

The *wt1* gene was isolated from the region of human chromosome 11p13 implicated in predisposition to the development of Wilms tumor (*1, 2*). The expression pattern of WT1, detection of intragenic deletions, and point mutations suggest that this gene functions in the regulation of kidney and gonadal development and in the genesis of Wilms tumor (*3*). The zinc fingers in the WT1 protein are related to those of the early growth response (EGR) family of proteins, and WT1 binds to a consensus DNA

Medical Research Council Human Genetics Unit, Western General Hospital, Edinburgh, EH4 2XU, Scotland.

*To whom correspondence should be addressed.

binding site for these proteins (*4*).

Studies of EGR1 and EGR2 (*5, 6*) showed that each finger contacts a 3-bp subsite of DNA antiparallel to the guanine (G)-rich strand of the double helix, so that the most COOH-terminal finger contacts the 5' end of the binding site. Amino acids in the NH_2-terminal portion of the α helix of each finger contact G residues in the DNA. The amino acid preceding the α helix of each finger (Fig. 1A, box I) contacts the third base of the subsite ($- - G$). In EGR1 finger 2, the third residue of the α helix (Fig. 1A, box II) contacts the second base ($- G -$), and in fingers 1 and 3 the sixth residue (Fig. 1A, box III) contacts the first base ($G - -$). It appears that the

binding site for an EGR-type zinc finger protein can be deduced from this simple recognition code. Other nucleotide residues seem to be of little importance in determining binding specificity, although it seems unlikely that proteins with identical contact residues (for example, EGR1, EGR2, and EGR4) fulfill their respective cellular functions by binding identical DNA targets in vivo (*7*). Fingers 2 through 4 of WT1 bind to the EGR1 consensus site (*4*). However, WT1 contains an extra finger not found in other EGR-like proteins (Fig. 1A) whose function in determining binding specificity is not understood.

The *wt1* gene is atypical in another respect. In other EGR-like proteins, seven amino acids separate adjacent fingers, and these may be important in juxtaposing adjacent fingers correctly relative to the target (*6*). In WT1 use of an alternative 5' splice junction introduces three extra amino acids (KTS) between fingers 3 and 4 (Fig. 1, A and B). This is in fact the predominant form of human and murine WT1 mRNA in all cells that express WT1 (*8*), and we refer to it here as the +KTS form of WT1. These extra amino acids may displace the fourth zinc finger relative to the EGR binding site, and indeed the +KTS form of WT1 is unable to bind this sequence (*4, 9*). Because its conservation and cellular abundance suggest that the +KTS form of WT1 has an in vivo function, we have tested whether zinc fingers of the +KTS form bind to DNA sequences other than the EGR binding site.

We identified binding sites, from the human genome, for both forms of the WT1 zinc fingers, with whole-genome polymerase chain reaction (PCR) (*10*). The zinc fingers from both the +KTS and −KTS forms of WT1 were expressed as β-galactosidase (β-gal) fusion proteins (Fig. 1B) (*11*) and bound in vitro to human DNA, converted to a form suitable for amplification by PCR by ligation to catch-linkers (*12*). After multiple rounds of binding, the amplified DNA was cloned and sequenced. Clones derived from this procedure fell into two distinct classes depending on the splice form of WT1 used (Fig. 2A). Clones isolated with the −KTS form of WT1 contained runs of GT dinucleotides, as found in the $(CA)_n$ class of repeated DNA sequence. Such sequences can present G residues in many of the correct positions for contact with EGR-type zinc fingers. Electrophoretic mobility-shift assays were performed on the whole-genome PCR clones (Fig. 2B) (*13*). The $(GT)_n$-containing clones showed reduced mobility with the form of WT1 (−KTS) used in their isolation (Fig. 2B). As judged by competition experiments, the binding affinity of −KTS WT1 for these sequences is at least four-